

## Feature Article

# Ethylene oligomerization in zeolite-grafted Cr(III)-diphosphinoamine catalysts using triisobutylaluminium as cocatalyst: Change from dimerization to trimerization due to confinement effect



Huaiqi Shao<sup>a</sup>, Jingjing Wang<sup>a</sup>, Ruofei Wang<sup>a</sup>, Liwu Song<sup>a</sup>, Xiaoyan Guo<sup>b</sup>, Tao Jiang<sup>a,\*</sup>

<sup>a</sup> Tianjin Key Laboratory of Marine Resources and Chemistry, College of Chemical Engineering and Materials Science, Tianjin University of Science & Technology, Tianjin 300457, PR China

<sup>b</sup> Key Laboratory of Pollution Processes and Environmental Criteria (Nankai University), Ministry of Education, Tianjin Key Laboratory of Environmental Remediation and Pollution Control, College of Environmental Science and Engineering, Nankai University, Tianjin 300457, PR China

## ARTICLE INFO

## Keywords:

Ethylene oligomerization  
Confinement effect  
Ethylene trimerization  
Heterogeneous catalyst

## ABSTRACT

Zeolite-supported Cr(III)-diphosphinoamine (Cr(III)-PNP) catalysts were prepared through grafting PNP on HY and NaY zeolites followed by complexing with  $\text{CrCl}_3(\text{THF})_3$  for ethylene oligomerization. The structure of supported Cr(III)-PNP catalysts was characterized by scanning electron microscopy, X-ray diffraction, nitrogen adsorption and desorption, thermogravimetric analyses and Fourier transform infrared, and the influence of the supported pattern on reactivity for ethylene oligomerization were investigated. The results revealed that the complex of Cr(III)-PNP was grafted on silicon hydroxyls in the pore channel of HY zeolite to decrease pore size but to maintain pore structure. Comparing with homogeneous Cr(III)-PNP producing 1-butene as main product, HY-supported catalyst had higher activity and selectivity toward 1-hexene increased from 4.07% to 73.24% using triisobutylaluminium as cocatalyst. The increase is attributed to confinement effect of the pore channel, which increases the stability of the chromacycloheptane intermediate to 1-hexene. The confinement effect for ethylene oligomerization was revealed in experiment.

## 1. Introduction

Linear  $\alpha$ -olefins, such as 1-hexene and 1-octene, are important intermediates for producing linear low-density polyethylene (LLDPE) as co-monomers [1,2]. The present technologies for producing linear  $\alpha$ -olefins are mostly based on ethylene oligomerization, resulting in a mathematical product distribution like Schulz-Flory or Poisson, which require purification through fractional distillation [3]. Thus, the continually increasing demands for 1-hexene and 1-octene have led to interest in more-selective oligomerization technologies.

Manyik et al. discovered the selective trimerization of ethylene to 1-hexene using homogeneous chromium 2-ethylhexanoate activated by partially hydrolyzed triisobutylaluminium [4], and then Briggs improved this system by the addition of dimethoxyethane with selectivity for ethylene oligomerization to 1-hexene (74%) [5]. A mechanism involving chromacycloheptane intermediate was proposed and accepted as mechanism of selective ethylene trimerization [4,5]. In 2002, the diphosphinoamine (PNP) ligands were reported as very successful architecture in combination with a soluble chromium source and methylaluminumoxane for the selective trimerization of ethylene to 1-hexene

(90%) [6]. A few years later, by removing *ortho*-substitution from the aryl groups of PNP, researchers from Sasol discovered a catalytic system of selective tetramerization of ethylene to 1-octene (70%), and a mechanism of chromacyclononane intermediate was postulated [7,8]. Follow-up work focused on reaction kinetics, chromium species, ligands and cocatalyst to investigate reaction mechanism and to improve the reactivity and selectivity toward  $\alpha$ -olefins [9–12]. Among them, a number of heterogeneous catalyst systems for ethylene trimerization and tetramerization were reported, and then the confinement effect was investigated to improve the reactivity [13–16].

The confinement effect in microporous catalyst has been widely accepted [17,18], but influence of this effect on reaction performance for ethylene oligomerization has been rarely studied and is still unclear [14–16]. Monol et al. reported a heterogeneous trimerization catalyst based on  $\text{Cr}[\text{N}(\text{SiMe}_3)_2]_3$  and isobutylaluminumoxane supported on silica, which gave an overall 1-hexene selectivity of 74.2% and an activity of 3170 g/mmol Cr per hour, and unsupported catalyst had the activity decreased to about 1/800 [13]. Toulhoat and co-authors used grand canonical Monte Carlo simulations to investigate the confinement effect within zeolitic structures on the activity and selectivity of ethylene

\* Corresponding author.

E-mail address: [jiangtao@tust.edu.cn](mailto:jiangtao@tust.edu.cn) (T. Jiang).

<http://dx.doi.org/10.1016/j.apcata.2017.07.021>

Received 10 May 2017; Received in revised form 10 July 2017; Accepted 13 July 2017

Available online 14 July 2017

0926-860X/ © 2017 Elsevier B.V. All rights reserved.

oligomerization, using a  $(\eta^5\text{-C}_5\text{H}_4\text{CMe}_2\text{C}_6\text{H}_5)\text{TiCl}_3$  catalyst for ethylene trimerization, which was confined in zeolite through Van der Waals' force. Their result predicted that selectivity toward 1-hexene decreased and selectivity toward 1-octene increased with increasing pore size, and the suitable pore size for producing 1-octene was approximately 1 nm, in which pore the chromacyclononane was more stable [14].

In our previous work,  $\text{Cr}(\text{acac})_3/\text{PNP}$  were supported on MAO-treated HY and NaY to investigate confinement effect for ethylene oligomerization. The results showed that NaY-supported  $\text{Cr}(\text{acac})_3/\text{PNP}$  catalyst had weak confinement effect on increasing selectivity toward 1-octene, and detailed reason was not revealed yet, because the catalyst structure was difficult to be analyzed clearly [15,16]. In this work, we prepared zeolite-supported Cr(III)-PNP catalysts through grafting Cr(III)-PNP on HY and NaY zeolites to obtain catalysts with clear structure for investigating confinement effect. The structure of these supported catalysts was characterized and reaction performance for ethylene oligomerization was presented.

## 2. Material and methods

### 2.1. Materials

Tris(tetrahydrofuran) chromium trichloride ( $\text{CrCl}_3(\text{THF})_3$ ), 3-aminopropyltriethoxysilane, chlorodiphenyl phosphine and chlorotrimethylsilane were purchased from J&K Co. HY and NaY zeolites were purchased from Nankai University Catalyst Co. Methylaluminoxane (MAO) (toluene solution of  $1.4 \text{ mol L}^{-1}$ ), triethylaluminum (TEA) and triisobutylaluminum (TIBA) (toluene solution of  $1.1 \text{ mol L}^{-1}$ ) were purchased from Aldrich. Polymerization-grade ethylene was obtained from Tianjin Summit Specialty Gases Co. Cyclohexane and toluene were dried and degassed prior to use. All other chemicals were obtained commercially and used as received.

### 2.2. Preparation of supported catalysts

Preparation process of zeolite-supported Cr(III)-PNP catalyst was shown in Scheme 1.

$(\text{Ph}_2\text{P})_2\text{N}(\text{CH}_2)_3\text{Si}(\text{OCH}_2\text{CH}_3)_3$  was synthesized referring to the method described in the literature [19]. 3-Aminopropyltriethoxysilane (7.0 mL, 30.0 mmol), triethylamine (9.2 mL, 66.0 mmol) were dissolved in 120 mL of toluene in a two-neck flask under nitrogen. The solution was cooled to  $-40^\circ\text{C}$  and  $\text{Ph}_2\text{PCl}$  (11.2 mL, 60.0 mmol) was

added dropwise in 1 h. The solution was warmed up to room temperature and further stirred for 2 h. The mixture was filtered and the solid was washed with a mixture of toluene (20 mL) and ether (20 mL). The solution was merged and solvent was removed under reduced pressure. The residue was recrystallized with ethanol to obtain a white powder assigned as PNP.  $^{31}\text{P}$  NMR( $\text{CDCl}_3$ ):62.5(s).  $^1\text{H}$  NMR( $\text{CDCl}_3$ ):  $\delta = 0.22$  (t, 2H,  $^3J(\text{H,H}) = 8.3 \text{ Hz}$ ;  $-\text{CH}_2\text{Si}$ ), 1.08–1.24 (m, 9H;  $-(\text{CH}_3)_3$ ), 1.42 (m, 2H;  $-\text{CH}_2-\text{CH}_2\text{Si}$ ), 3.20 (m, 2H;  $-\text{CH}_2\text{N}$ ), 3.60 (m, 6H;  $-\text{Si}(\text{OCH}_2-)_3$ ), 7.26–7.40 (m, 20H;  $-\text{PPh}_2$ ).

HY zeolite was pretreated at  $100^\circ\text{C}$  for 10 h at  $-0.095 \text{ MPa}$  of pressure then stored in glove box until required. HY (5.0 g) and the PNP (1.0 g) were charged in a flask in a glove box, and the sealed flask was removed from glove box. Toluene (50 mL) was added to the flask. The stirred mixture was heated up to  $110^\circ\text{C}$  and then refluxed for 12 h. The solid was washed with toluene ( $3 \times 30 \text{ mL}$ ) and dried under vacuum to give the HYPNP.

HYPNP (4.0 g) was suspended in toluene (10 mL), and chlorotrimethylsilane (20.0 mL) was added dropwise at  $30^\circ\text{C}$  under nitrogen. The mixture was kept for 6 h until filtration. The solid was washed three times with toluene ( $3 \times 30 \text{ mL}$ ) and then dried under vacuum to obtain HYPT.

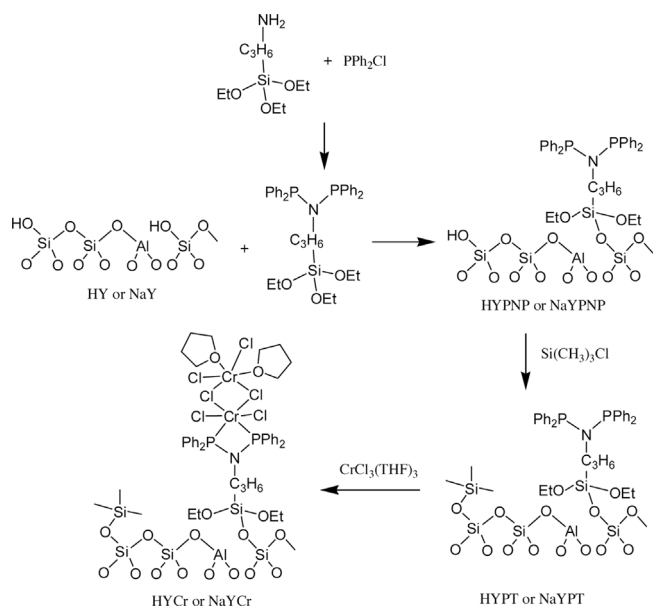
3.0 g of HYPT was charged in a flask and suspended in toluene (10 mL) and then a solution of  $\text{CrCl}_3(\text{THF})_3$  (0.37 g, 1.0 mmol) in toluene (40 mL) was added dropwise in 30 min under nitrogen. The mixture was heated at  $50^\circ\text{C}$  for 12 h until filtration. The solid was washed three times with 30 mL of toluene and then dried under vacuum at  $50^\circ\text{C}$  to obtain HYCr. NaY-supported Cr(III)-PNP catalyst was prepared using similar procedure and assigned as NaYCr.

### 2.3. Characterization of supports and catalysts

Scanning electron microscopy (SEM) images were obtained using a Hitachi SU1510 instrument operated at an accelerating voltage of 5 kV. X-ray diffraction (XRD) patterns were recorded using a Rigaku RINT2000 diffractometer operated at 40 kV and 40 mA, using  $\text{CuK}\alpha$  radiation. The chromium content of the supported catalyst was determined using a Agilent 7500 inductively coupled plasma mass spectrometer (ICP-MS). Nitrogen adsorption and desorption isotherms were measured at  $-196^\circ\text{C}$  using a Quantachrome autosorb (iQ) apparatus. Samples were first degassed at  $300^\circ\text{C}$  for 4 h (zeolite) or at  $60^\circ\text{C}$  for 12 h (supported catalyst). Specific surface areas ( $S_{\text{BET}}$ ) were calculated using the Brunauer-Emmett-Teller (BET) method. Pore size distributions and pore diameters ( $D_p$ ) were calculated using the non local density functional theory method (NLDFT). The total pore volumes ( $V_p$ ) were determined from the adsorption volume at a value of  $P/P_0$  of 0.995. Micropore surface areas ( $S_{\text{micro}}$ ) and volumes ( $V_{\text{micro}}$ ) were calculated using the  $t$ -plot method. Thermogravimetric analyses were performed using a STA449F5 system (TG-DSC, Netzsch) operated at a heating rate of  $10^\circ\text{C min}^{-1}$  up to  $700^\circ\text{C}$  under a flow of  $\text{N}_2$  ( $60 \text{ mL min}^{-1}$ ). Fourier transform infrared (FTIR) spectra were recorded using a Bruker Tensor 27 instrument. The sample was mixed with KBr powder and then was pressed to a disc in glove box. The sample disc was stored under nitrogen until characterization.

### 2.4. Ethylene oligomerization and products analysis

Ethylene oligomerization was performed in a 0.5-L autoclave. After evacuation and flushing with  $\text{N}_2$  (three times) and then ethylene (twice), the autoclave was charged with cyclohexane (0.1 L), which was stirred mechanically under ambient ethylene atmosphere. When the desired reaction temperature was reached, cocatalyst (MAO, or TEA, or TIBA) and the supported catalyst suspended in cyclohexane (5 mL) were injected into the reactor. Typically, after 30 min the mixture was cooled rapidly to  $-20^\circ\text{C}$  and slowly vented, and then the reaction was quenched through the addition of a solution of HCl in EtOH (10 wt.%). The catalyst activity was calculated from the increase in product mass.



Scheme 1. Preparation of Cr(III)-PNP catalysts supported on HY and NaY zeolites.

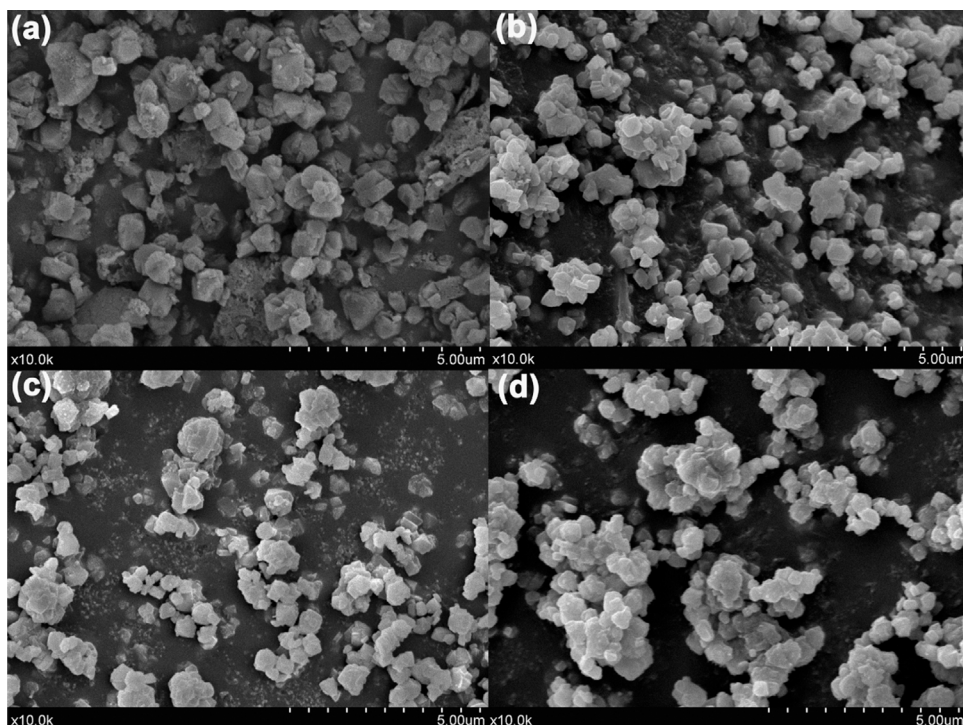


Fig. 1. Morphologies of HY(a), HYCr(b), NaY(c) and NaYCr(d).

All experimental were repeated at least two times, and activity error and selectivity error of main product less than 10% were accepted.

The product was sealed and analyzed as quickly as possible through gas chromatography (GC) using a Agilent 7890A instrument equipped with an HP-5 capillary column. The sample was maintained at 35 °C for 10 min, heated at 10 °C min<sup>-1</sup> until the temperature reached 280 °C, and then maintained at that temperature for 10 min.

### 3. Results and discussion

#### 3.1. Characterization of the catalyst structure

Fig. 1 displays the morphologies of the zeolites and the zeolite-supported Cr(III)-PNP catalysts. After supporting chromium on HY zeolite, the particle size and the pattern of outside surface are kept almostly constant, accompanying with breaking and recombination of a small amount of particles. The results suggest that the chromium is mainly loaded into the pore channel so that the pattern of outside surface is kept. Comparing with HYCr catalyst, the particles of NaYCr catalyst present agglomeration.

XRD patterns of the zeolites and the zeolite-supported Cr(III)-PNP catalysts are presented in Fig. 2. After grafting Cr(III)-PNP on HY and NaY, the crystal structures of the zeolites are maintained, as evidenced by the absence of changes in diffracted angles and intensities [20]. A small shoulder peak at 15.3° can be attributed to {331} crystal plane of CrCl<sub>3</sub> crystal for HYCr and NaYCr (JCPDS card no.32-0279), although other characteristic peaks of CrCl<sub>3</sub> crystal are overlapped by diffracted peaks of the zeolites. Comparing with HYCr catalyst, stronger peak at 15.3° of CrCl<sub>3</sub> is presented on NaYCr catalyst.

The different supported patterns of Cr(III)-PNP supported on HY and NaY are also evident from the different changes in the pore structures. After grafting Cr(III)-PNP, the obviously different pore structures are presented on HYCr and NaYCr (see Table 1 and Fig. 3). Relative to its support, HYCr decreases in its values of  $S_{\text{micro}}$ ,  $V_{\text{micro}}$  and  $D_p$  of 546.975 m<sup>2</sup>/g, 0.202 cm<sup>3</sup>/g and 0.35 nm, respectively, suggesting main change is presented in the micro pore. The shape of isotherms is maintained but the adsorption volume is obviously decreased (see Fig. 3), and the distribution of pore size becomes narrower. Such results

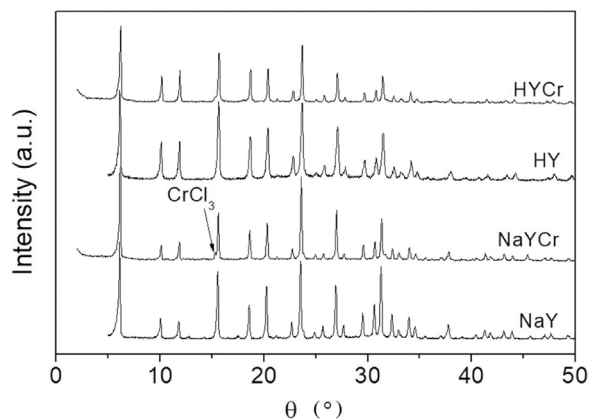


Fig. 2. XRD patterns of zeolites and zeolite-supported catalysts.

suggest that the loading mainly fills into the micropores, because hydroxyls, reacting with silicon hydroxyl of PNP ligand, mainly locate in the pore channel. Differently, smaller change of  $S_{\text{micro}}$  and  $V_{\text{micro}}$  and no change of pore size are presented on NaYCr catalyst. In combination with the results from XRD, it can be determined that chromium is mainly loaded on the outside of the particle and in the pore of NaY, although NaYCr has nearly the same amount of chromium loaded, comparing with HYCr. It is possible that stronger acidity of HY zeolite promotes the grafting reaction between PNP and hydroxyl to increase the loading of PNP, which evidence is supported by results of nitrogen distribution on HYCr and NaYCr from EDS results, shown in Fig. A1 in the supplementary. The HCl formed in the treating process by using chlorotrimethylsilane can destroy the PNP ligand, and more likely, it can form salt with N in PNP to decrease the ability complexed with CrCl<sub>3</sub>(THF)<sub>3</sub>. Fortunately, the amount of formed HCl was small (see Fig. A1 in the supplementary), so the unfavorable effect on the complexing performance was small. In the supported process no extra acid was added to avoid the condensation between PNP molecules. Chromium is presented as Cr(III) according XPS result (binding energy of Cr<sub>3p/2</sub> is 577.6 eV, see Fig. A2 in the supplementary). The distance between two chromium molecules is larger than the pore size. In fact the distance is

**Table 1**  
Properties of zeolites and zeolite-supported catalysts.

Samples	Content of Cr (wt.%)	$S_{\text{BET}}$ ( $\text{m}^2/\text{g}$ )	$S_{\text{micro}}$ ( $\text{m}^2/\text{g}$ )	$V_{\text{p}}$ ( $\text{cm}^3/\text{g}$ )	$V_{\text{micro}}$ ( $\text{cm}^3/\text{g}^1$ )	$D_{\text{p}}$ (nm)	Distance between two chromium <sup>a</sup> (nm)
HY	–	1011.068	970.785	0.453	0.367	1.17	–
NaY	–	1016.794	1000.499	0.429	0.376	1.11	–
HYCr	0.80	444.216	423.810	0.265	0.165	0.82	2.2
NaYCr	0.81	773.915	766.643	0.361	0.294	1.11	2.9

<sup>a</sup> Calculated according with content of chromium and specific surface area.

larger than the above size due to the existence of the crystal  $\text{CrCl}_3$ , so the chromium molecules should be located in a different cage of the zeolite.

The interaction between the support and Cr(III)-PNP is investigated by using TG-DSC. Fig. 4 displays the thermograms of  $\text{CrCl}_3(\text{THF})_3$ , the PNP and the zeolite-supported catalysts. According to weight loss for  $\text{CrCl}_3(\text{THF})_3$ , the peaks at 142 °C and 293 °C can be attributed to decomposition of THF and Cr-Cl bonds, respectively. For the PNP ligand, the exothermic peak at 75 °C without weight loss suggests that is peak of crystal transformation of the PNP. A large weight loss at 374 °C is caused by the decomposition of other bonds besides Si–O bonds in the PNP. For HYPNP, the exothermic peak at 102 °C can be caused by volatilization of residual toluene, and the exothermic peak at 422 °C is attributed to decomposition of the PNP, which temperature is raised by 48 °C, comparing with the free PNP ligand. This temperature raise reveals the existence of chemical bond between the PNP and the zeolite. In the TG-DSC trace for HYCr, the exothermic peaks at 123 °C, 266 °C and 413 °C can be attributed to decomposition of THF, break of Cr-N bonds of Cr(III)-PNP and followed decomposition of the PNP. By comparison, the broad peak at 307 °C for NaYCr catalyst can attributed to combination of break of Cr-N bonds, break of Cr-Cl of the  $\text{CrCl}_3$  and decomposition of the PNP. Such results mean that different supported state is presented on HYCr and NaYCr catalysts.

Next, FTIR spectroscopy is used to characterize the interactions between Cr(III)-PNP and the support (Fig. 5). For the PNP ligand, the peaks at  $1166\text{ cm}^{-1}$ ,  $1077\text{ cm}^{-1}$  and  $865\text{ cm}^{-1}$  can be attributed to stretching vibrations of C–N bond, Si–O–C bond and Si–C bond. Relative to the signals in the FTIR spectrum of HY, the vibrations of the inner Si–O tetrahedra of HYCr shift from  $1043$  and  $804\text{ cm}^{-1}$  to  $1046$  and  $804\text{ cm}^{-1}$ , respectively, and the bending vibration of dicyclo framework shifts from  $580\text{ cm}^{-1}$  to  $584\text{ cm}^{-1}$ . These little shifts suggest that supporting of Cr-PNP has little effect on the structures of HY [21]. The peak at  $856\text{ cm}^{-1}$  can be attributed to bending vibration of C–O–C in THF [22]. Similar results are presented on NaYCr.

### 3.2. Reaction performances

The influences of reaction time on the activity of ethylene oligomerization on  $\text{CrCl}_3(\text{THF})_3/\text{PNP}$  and HYCr catalysts presented in Fig. A3 in the supplementary show that the activities decrease after 30 min on homogeneous Cr(III)/PNP and after 20 min on HYCr, respectively.

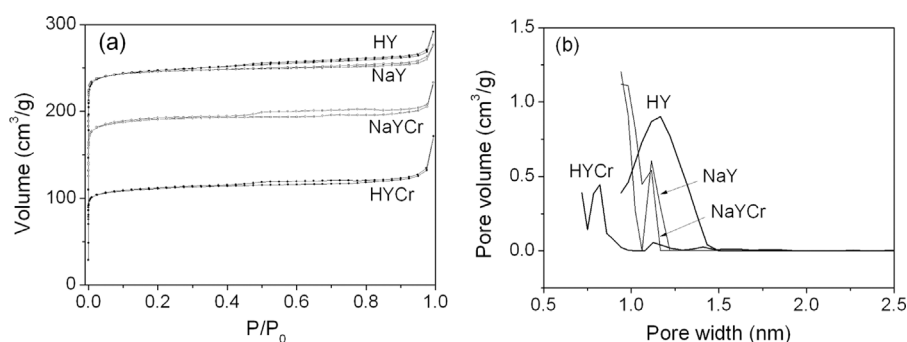


**Fig. 3.** Isotherms(a) and pore size distributions(b) of zeolites and zeolite-supported catalysts.

Such results show that earlier deactivation is presented on HYCr. It is possible that the formed PE hinders the pore channel for ethylene transfer.

Table 2 presents the reactivities and product distributions of homogeneous  $\text{CrCl}_3(\text{THF})_3/\text{PNP}$  and the zeolite-supported Cr(III)-PNP catalysts for ethylene oligomerization. For  $\text{CrCl}_3(\text{THF})_3/\text{PNP}$  catalyst with MAO as cocatalyst, the 1-octene is main product in agreement with the Blamm's result with  $(\text{Ph}_2\text{P})_2\text{N}(\text{CH}_2)_3\text{Si}(\text{OCH}_3)_3$  as ligand [23]. Differently, 1-butene and 1-hexene are main products using TEA and TIBA as cocatalysts, and meanwhile, the activities of ethylene oligomerization are rapidly decreased. The products distribution means that oligomerization acts up on the metallocyclic mechanism [5]. Comparing with  $\text{CrCl}_3(\text{THF})_3/\text{PNP}$  catalyst with MAO as cocatalyst, HYCr and NaYCr catalysts present lower activities and broader product distributions. In contrast, the activities are rapid decreased by using TEA and TIBA as cocatalysts, while 1-hexene becomes main product for TIBA, and 1-hexene and 1-octene become main products for TEA. In general, the influence of activity affected by supported process may be attributed to: (i) change of the state of the active sites after supporting; (ii) the steric hindrance of pore wall on accessibility of cocatalyst to the active sites; (iii) restriction of ethylene access to the active sites, thereby hindering the ethylene insertion [24]. Among them, the MAO with large volume cannot enter into small pore of zeolite, so that chromium is not enough activated, causing activities decreased and product distributions changed for HYCr and NaYCr [25]. HYCr has more selectivity toward 1-hexene than NaYCr, because of the difference of the active site distribution (see Figs. 2 and 4), and  $\text{CrCl}_3$  is active less.

The catalytic performances of  $\text{CrCl}_3(\text{THF})_3/\text{PNP}$  for ethylene oligomerization in the presence of zeolite were presented in Table 2 (see entry 2, 4 and 6). In the presence of zeolite, the  $\text{CrCl}_3(\text{THF})_3/\text{PNP}$  using MAO, TEA or TIBA as cocatalysts presents similar activity with homogeneous  $\text{CrCl}_3(\text{THF})_3/\text{PNP}$  catalyst. This result means that performance of the alkylaluminium and aluminoxane is presented slight change. It is possible that the amount of zeolite is too small (about 30 mg, equal to amount of HYCr in entry 10) and does not lead obvious modification of alkylaluminium. The selectivity toward 1-octene using MAO as cocatalyst increases obviously, and 1-hexene becomes main product using TEA and TIBA as cocatalysts in the presence of HY zeolite. Change of main product might be caused by the confinement effect in accordance with Toulhoat's calculating results.

According to Toulhoat's result, the zeolite having pore size of

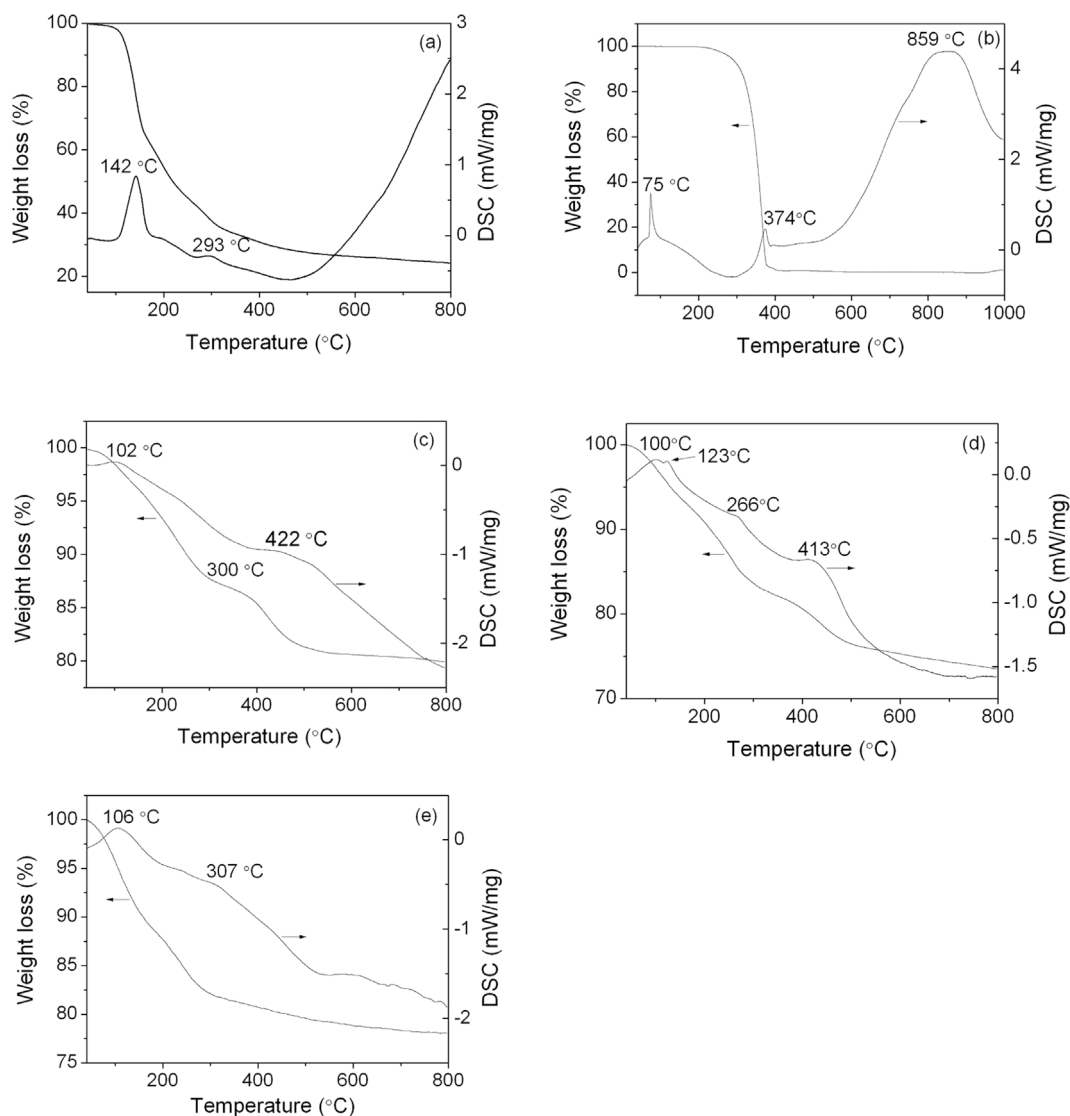


Fig. 4. Thermogravimetric curves of  $\text{CrCl}_3(\text{THF})_3$ (a), PNP(b), HYPNP(c), HYCr(d) and NaYCr(e).

approximately 1 nm would increase the production of 1-octene due to the confinement effect of pore channel [14]. However, MAO as most effective cocatalyst for usual Cr-PNP catalyst system has kinetic diameter of greater than 1 nm, so confinement effect could not be checked in our present work (entry 7 and 8). In this work, ethylene trimerization is presented over HYCr (entry 10 and 12), instead of ethylene dimerization over homogeneous  $\text{CrCl}_3(\text{THF})_3/\text{PNP}$  catalyst (entry 5). The oligomerization reaction, changed from dimerization to trimerization, may be caused by change of the active state or confinement effect. Because the chromium active site is far enough from bonding position of the PNP on the support though Si-O-Si bond, so the change of the active state might be insignificant, so the confinement effect is likely to be crucial. The pore size of HYCr is 0.82 nm, so the ethylene trimerization to 1-hexene becomes main reaction. Such results are according with calculated regularity by Toulhoat.

The reactivity of in situ HYPNT and  $\text{CrCl}_3(\text{THF})_3$  was investigated for ethylene oligomerization (entry 13), similar with proposed method by Toulhoat [14]. Comparing with homogeneous  $\text{CrCl}_3(\text{THF})_3/\text{PNP}$ , the similar activity is presented, and 1-hexene becomes main product. In the presence of porous HYPNT,  $\text{CrCl}_3(\text{THF})_3$  can coordinate with PNP in the pore to catalyze ethylene trimerization. Comparing with HYCr catalyst, insufficiently confinement effect is presented, because of insufficient formation of Cr-PNP complex, being consistent with our previous work [15]. Jabri et al. investigated the Cr-Al species of PNP/

$\text{CrCl}_3$  with  $\text{AlMe}_3$  cocatalyst through X-ray Crystallography [10]. Their results showed that new divalent catalyst precursor was formed and subsequently activated by MAO for ethylene oligomerization to produce 1-hexene and 1-octene. In our work, the divalent catalyst with similar structure is difficult to be formed due to the immobilization of the PNP ligand. Mononuclear chromium active site activated by TIBA is formed and catalyzes ethylene trimerization to 1-hexene (entry 10 and 12 in Table 2).

The influences of the reaction condition on catalytic reactivity over HYCr are presented in Table 3. The catalytic activity increases initially with increasing temperature and reaches a maximum at 45 °C, and then decreases from 45 to 65 °C. The elevated temperature can decrease ethylene solubility in solvent and increase deactivation rate of the active sites, although the elevated temperature is expected to result in overall higher propagation and transfer rates of ethylene. It is combination of these effects that is likely to account for the observed temperature dependence of the activity. The change trend of selectivity toward 1-hexene is according with change trend of the activity. It indicates that the rate of chain transfer, particularly  $\beta$ -H elimination, increases more than the rate of propagation below 45 °C [26]. The productions of higher  $\alpha$ -olefins (> C6) increase with increasing temperature above 45 °C.

Improving ethylene pressure dramatically increases the catalytic activity and the selectivity toward 1-octene, and decreases the

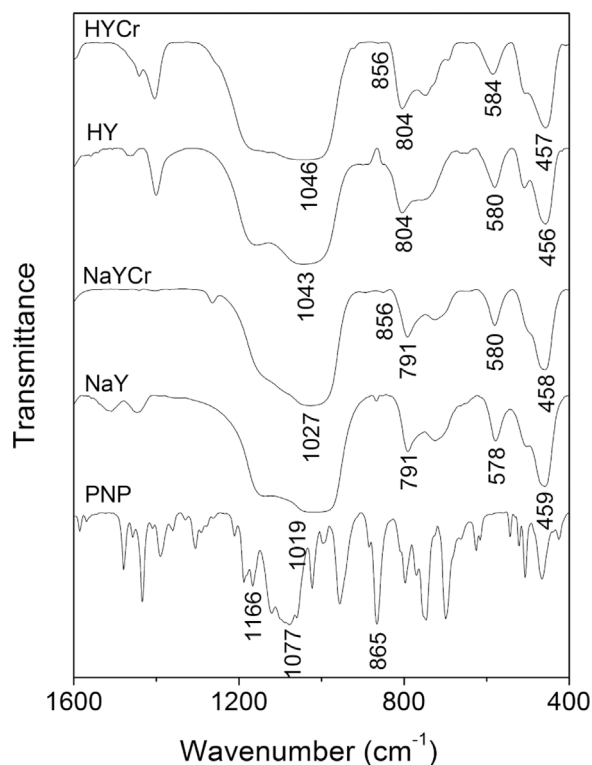


Fig. 5. FTIR spectra of PNP, zeolites and zeolite-supported catalysts.

selectivities toward 1-butene and 1-hexene. This result shows that the elevated pressure leads to an increase of ethylene solubility, which results in the increase of chain propagation rate and thus induces the increase of catalytic activity and selectivity toward 1-octene [27]. The dynamic regularity of ethylene oligomerization on the zeolite-supported Cr(III)-PNP is similar with normal Cr(III)/PNP catalyst for ethylene tetramerization, on which catalyst the selectivity toward 1-octene is increased with ethylene pressure [26]. The previous results presented that the reaction rate was dependent on ethylene concentration in the order of 2 for ethylene trimerization over homogeneous Cr(2-EH)<sub>3</sub> catalyst [4] and in the order of 1.57 for ethylene

tetramerization using Cr(acac)<sub>3</sub>/PNP/MAO catalyst system [9]. However, reaction order on ethylene pressure is far less than 2 on HYCr catalyst (about 0.17 calculated from Table 3). This result means that the restriction of the pore channel on ethylene transfer is very obvious, and ethylene transfer across pore channel may be rate-determining step affecting the activity.

The catalytic activity and selectivity toward 1-octene first increase with Al/Cr ratio and decrease thereafter. In contrast, the selectivity toward 1-hexene reach a maximum at Al/Cr ratio of 400, meaning the activated chromium state at this Al/Cr ratio is most suitable for ethylene trimerization. The alkylaluminium can activate chromium sites to form appropriate activated state, but excess amount of alkylaluminium may interfere with the formation of the active chromium species by the over-reduction of chromium species.

#### 4. Conclusion

The complex of Cr(III)-PNP is mainly grafted into the pore channel of HY zeolite and in pore channel and outside of pore of NaY zeolite due to the difference of the acidity of zeolites. The different supported pattern affects the reactivity of ethylene oligomerization. The selective trimerization of ethylene is presented on HY-supported Cr(III)-PNP catalyst using TIBA as cocatalyst, and broader product distribution is presented on NaY-supported one. HY-supported Cr(III)-PNP catalyst has higher activity for ethylene oligomerization than homogeneous one, while main product becomes from 1-butene to 1-hexene. The change of the selectivity can be attributed to the confinement effect of pore channel of supported catalyst to increase stability of chromacycloheptane intermediate for 1-hexene. The confinement effect for ethylene trimerization in the agreement of Toulhoat's theory is confirmed in experiment. In the future, the more effort will be focused on the construction of heterogeneous Cr-based catalyst with regular structure for investigating confinement effect in ethylene tetramerization.

#### Acknowledgments

This study was supported by the National Key Research and Development Program of China (2017YFB0306700), the Natural Science Foundation of Tianjin City (14JCYBJC23100, 15JCYBJC48100 and 16JCZDJC31600).

Table 2

Catalytic activity and selectivity of zeolite-supported catalysts.

Entry	Catalyst	Cocatalyst	Activity (10 <sup>5</sup> g/(mol Cr·h))	Product <sup>c</sup> (wt.%)								
				1-C <sub>4</sub> <sup>=</sup>	C <sub>6</sub>	1-C <sub>6</sub> <sup>=</sup> (in C <sub>6</sub> )	C <sub>cyclus</sub> (in C <sub>6</sub> )	C <sub>8</sub>	1-C <sub>8</sub> <sup>=</sup> (in C <sub>8</sub> )	C <sub>10</sub>	1-C <sub>10</sub> <sup>=</sup> (in C <sub>10</sub> )	> C <sub>10</sub>
1	PNP + CrCl <sub>3</sub> (THF) <sub>3</sub>	MAO <sup>a</sup>	59.0	1.07	15.98	41.52	52.02	55.02	95.10	5.33	42.12	22.6
2	PNP + CrCl <sub>3</sub> (THF) <sub>3</sub> + HY	MAO <sup>a</sup>	51.3	3.61	21.76	58.00	31.33	69.41	96.46	2.22	11.17	3.00
3	PNP + CrCl <sub>3</sub> (THF) <sub>3</sub>	TEA <sup>b</sup>	0.18	77.94	22.06	100.00	–	–	–	–	–	–
4	PNP + CrCl <sub>3</sub> (THF) <sub>3</sub> + HY	TEA <sup>b</sup>	0.16	34.45	56.62	93.74	2.36	1.74	98.32	2.73	17.85	4.46
5	PNP + CrCl <sub>3</sub> (THF) <sub>3</sub>	TIBA <sup>b</sup>	1.33	90.41	8.40	48.46	51.54	1.01	100.00	0.18	100.00	–
6	PNP + CrCl <sub>3</sub> (THF) <sub>3</sub> + HY	TIBA <sup>b</sup>	1.65	34.69	53.98	72.08	25.77	7.25	98.76	1.33	48.89	2.75
7	HYCr	MAO <sup>a</sup>	1.90	5.23	28.34	69.84	15.79	26.37	78.34	6.81	36.48	33.25
8	NaYCr	MAO <sup>a</sup>	1.82	3.86	28.94	68.32	30.47	31.29	72.34	3.67	56.22	32.42
9	HYCr	TEA <sup>a</sup>	3.85	7.97	49.03	86.49	5.28	36.26	82.47	6.74	29.08	–
10	HYCr	TIBA <sup>a</sup>	4.76	8.08	75.00	97.65	0.21	16.43	89.36	0.46	32.03	0.03
11	NaYCr	TIBA <sup>a</sup>	4.50	6.03	39.49	97.23	2.05	16.09	95.67	0.68	51.56	37.71
12	HYCr	TIBA <sup>b</sup>	2.51	13.48	82.34	64.30	30.15	3.60	60.57	0.30	32.15	0.28
13	HYPT + CrCl <sub>3</sub> (THF) <sub>3</sub>	TIBA <sup>b</sup>	1.70	20.60	54.01	54.03	22.40	16.00	71.88	0.54	42.53	8.85

<sup>a</sup> Reaction conditions: 4.8 μmol of Cr-based catalyst; pressure: 4 MPa; Al/Cr mole ratio = 400; temperature: 35 °C; solvent: cyclohexane; reaction time: 30 min.

<sup>b</sup> Reaction conditions: 4.8 μmol of Cr-based catalyst; pressure: 1 MPa; Al/Cr mole ratio = 400; temperature: 35 °C; solvent: cyclohexane; reaction time: 30 min.

<sup>c</sup> Oligomers analyzed by GC, and a small amount of polyethylene is not listed.

**Table 3**  
Influences of reaction condition on reaction activities and product distributions.

T (°C)	Pressure (MPa)	Al/Cr molar ratio	Activity <sup>a</sup> (10 <sup>5</sup> g/(mol Cr-h))	Product (wt.%)							
				1-C <sub>4</sub> <sup>=</sup>	C <sub>6</sub>	1-C <sub>6</sub> <sup>=</sup> (in C <sub>6</sub> )	C <sub>cyclics</sub> (in C <sub>6</sub> )	C <sub>8</sub>	1-C <sub>8</sub> <sup>=</sup> (in C <sub>8</sub> )	C <sub>10</sub>	> C <sub>10</sub>
45	4	400	9.76	5.46	80.83	99.26	0.56	11.81	96.26	1.82	0.08
55	4	400	4.30	4.87	67.08	88.64	4.79	18.63	70.62	2.63	6.79
65	4	400	2.64	3.25	53.64	92.65	3.24	20.16	82.26	4.67	18.28
35	3	400	4.52	9.14	76.34	85.63	13.62	10.64	76.34	1.02	2.86
35	2	400	4.23	11.23	79.82	73.68	20.15	8.34	66.89	0.23	0.38
35	4	500	4.19	6.32	52.13	92.34	4.35	14.76	90.26	3.64	23.15
35	4	300	4.26	5.15	53.12	98.14	1.03	27.03	98.32	0.29	14.41
35	4	200	3.02	4.30	65.34	35.67	45.23	22.77	72.87	0.27	7.32
35	4	100	2.10	3.77	67.89	40.21	55.68	16.34	78.67	0.16	11.84

<sup>a</sup> Reaction conditions: 2.4 μmol of HYCr catalyst; cocatalyst: TIBA; solvent: cyclohexane; reaction time: 30 min.

## Appendix A. Supplementary data

Supplementary data associated with this article can be found, in the online version, at <http://dx.doi.org/10.1016/j.apcata.2017.07.021>.

## References

- [1] J. Skupinska, Chem. Rev. 91 (1991) 613–648.
- [2] Y.V. Kissin, Polymers of higher olefins, Kirk-Othmer Encyclopedia of Chemical Technology, Wiley & Sons, Inc., 2005.
- [3] D.S. McGuinness, Chem. Rev. 111 (2011) 2321–2341.
- [4] R.M. Manyik, W.E. Walker, T.P. Wilson, J. Catal. 47 (1977) 197–209.
- [5] J.R. Briggs, J. Chem. Soc. Chem. Commun. 11 (1989) 674–675.
- [6] A. Carter, S.A. Cohen, N.A. Cooley, A. Murphy, J. Scutt, D.F. Wass, Chem. Commun. (2002) 858–859.
- [7] A. Bollmann, K. Blann, J.T. Dixon, F.M. Hess, E. Killian, H. Maumela, D.S. McGuinness, D.H. Morgan, A. Neveling, S. Otto, M. Overett, A.M.Z. Slawin, P. Wasserscheid, S. Kuhlmann, J. Am. Chem. Soc. 126 (2004) 14712–14713.
- [8] M.J. Overett, K. Blann, A. Bollmann, J.T. Dixon, D. Hassbroeck, E. Killian, H. Maumela, D.S. McGuinness, D.H. Morgan, J. Am. Chem. Soc. 127 (2005) 10723–10730.
- [9] R. Walsh, D.H. Morgan, A. Bollmann, J.T. Dixon, Appl. Catal. A: Gen. 306 (2006) 184–191.
- [10] A. Jabri, P. Crewdson, S. Gambarotta, I. Korobkov, R. Duchateau, Organometallics 25 (2006) 715–718.
- [11] Y. Shaikh, K. Albahily, M. Sutcliffe, V. Fomitcheva, S. Gambarotta, I. Korobkov, R. Duchateau, Angew. Chem. Int. Ed. 51 (2012) 1366–1369.
- [12] D.S. McGuinness, M. Overett, R.P. Tooze, K. Blann, J.T. Dixon, A.M.Z. Slawin, Organometallics 26 (2007) 1108–1111.
- [13] T. Monoi, Y. Sasaki, J. Mol. Catal. A: Chem. 187 (2002) 135–141.
- [14] H. Toulhoat, M.L. Fomena, T. de Bruin, J. Am. Chem. Soc. 133 (2011) 2481–2491.
- [15] H. Shao, Y. Li, X. Gao, C. Cao, Y. Tao, J. Lin, T. Jiang, J. Mol. Catal. A: Chem. 390 (2014) 152–158.
- [16] H. Shao, H. Zhou, X. Guo, Y. Tao, T. Jiang, M. Qin, Catal. Commun. 60 (2015) 14–18.
- [17] E.G. Derouane, J.M. André, A.A. Lucas, J. Catal. 110 (1988) 58–73.
- [18] T.K. Phung, L.P. Hernández, A. Lagazzo, G. Busca, Appl. Catal. A: Gen. 493 (2015) 77–89.
- [19] F. Schwyer-Tihay, P. Braunstein, C. Estournès, J.L. Guille, B. Lebeau, J.-L. Paillard, M. Richard-Plouet, J. Rosé, Chem. Mater. 15 (2003) 57–62.
- [20] Y. Huang, K. Wang, D. Dong, D. Li, M.R. Hill, A.J. Hill, H. Wang, Microporous Mesoporous Mater. 127 (2010) 167–175.
- [21] H. Xiao, X. Gao, D. Ding, S. Chen, Chin. J. Nonferr. Metals 9 (1999) 833–836.
- [22] A. Uusitalo, T.T. Pakkanen, E.I. Iiskola, J. Mol. Catal. A: Chem. 156 (2000) 181–193.
- [23] K. Blann, A. Bollmann, H. de Bod, J.T. Dixon, E. Killian, P. Nongodlwana, M.C. Maumela, H. Maumela, A.E. McConnell, D.H. Morgan, M.J. Overett, M. Prétorius, S. Kuhlmann, P. Wasserscheid, J. Catal. 249 (2007) 244–249.
- [24] C. Liu, T. Tang, B. Huang, J. Catal. 221 (2004) 162–169.
- [25] D.E. Babushkin, H.H. Brintzinger, J. Am. Chem. Soc. 124 (2002) 12869–12873.
- [26] T. Jiang, Y. Ning, B. Zhang, J. Li, G. Wang, J. Yi, Q. Huang, J. Mol. Catal. A: Chem. 259 (2006) 161–165.
- [27] S. Kuhlmann, J.T. Dixon, M. Haumann, D.H. Morgan, J. Ofili, O. Spuhl, N. Taccardi, P. Wasserscheid, Adv. Synth. Catal. 348 (2006) 1200–1206.